



Cite this: *Dalton Trans.*, 2016, **45**, 14265

Received 8th July 2016,
Accepted 28th July 2016

DOI: 10.1039/c6dt02709a

www.rsc.org/dalton

Copper(i) clusters with bulky dithiocarboxylate, thiolate, and selenolate ligands†

Pokpong Rungthanaphatsophon, Charles L. Barnes and Justin R. Walensky*

The coordination chemistry of copper has interest due to its use in biological systems as well as for photochemical and medicinal properties. We report the coordination chemistry of copper(i) complexes using terphenyl-based dithiocarboxylate, thiolate, and selenolate ligands. The number of metal ions of the resulting complexes can be tuned by varying the steric properties of the terphenyl ligands, changing the starting material, as well as adding PEt_3 . In addition, the steric crowding of the terphenyl ligand leads to varying reactivity. For example, while the reaction of carbon disulfide with $[\text{Cu}(2,6-(\text{Ph})_2\text{C}_6\text{H}_3)]_2$ results in an insertion into the copper–carbon bond, no reaction occurs with $[\text{Cu}(2,4,6-(\text{Mes})_2\text{C}_6\text{H}_3)]$, Mes = 2,4,6-Me₃C₆H₂, or $[\text{Et}_3\text{PCu}(2,4,6-(\text{Mes})_2\text{C}_6\text{H}_2)_2\text{C}_6\text{H}_3]$. The synthesis and characterization of new copper(i) complexes using NMR and IR spectroscopy, as well as X-ray crystallography is described.

Introduction

Copper has attracted attention due to its photochemical,¹ catalytic,^{2,3} and anti-microbial properties,⁴ as well as cytotoxicity.⁵ In nature, copper mainly occurs in the +1 and +2 oxidation states, and it is well known that copper(i) prefers to coordinate to soft donor ligands. Thus, the coordination chemistry of copper in nature is mainly dominated by amino acids such as histidine, cysteine, and methionine or ligands containing soft donor atoms such as sulfur.⁶ A variety of coordination numbers exist, ranging from two to five, and are predominantly linear, trigonal planar or tetrahedral geometries are observed. Copper-transporting proteins, such as eukaryote Atx1, are flexible in nature and feature copper in coordination numbers of two or three,⁷ while CusA a protein that is essential in bacteria for copper resistance,⁸ was found to contain one Cu(i) in a trigonal planar geometry, Fig. 1.

The enforcement of low coordination numbers can be achieved by having a ligand with large steric demand. The terphenyl-based ligand frameworks, Fig. 2, can provide such steric properties. Several derivatives of terphenyl ligands with nearly every main group element have been synthesized.⁹ Our interest was to use dithiocarboxylate, thiolate, and selenolate derivatives to produce copper(i) complexes to model the active site of copper-containing enzymes with linear, trigonal planar, or tetrahedral coordination geometries. We have previously

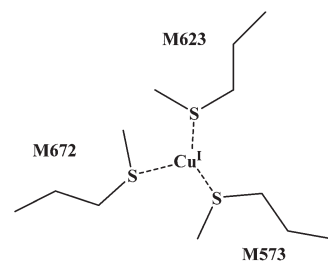


Fig. 1 Active site of CusA is shown.

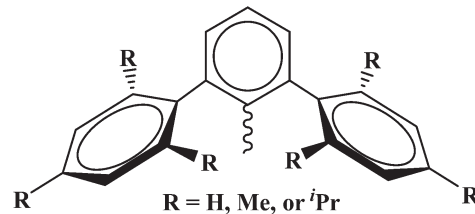


Fig. 2 General drawing of the terphenyl ligands used in this manuscript.

Department of Chemistry, University of Missouri, Columbia, MO 65211, USA.
E-mail: walenskyj@missouri.edu

† Electronic supplementary information (ESI) available. CCDC 1491737–1491749. For ESI and crystallographic data in CIF or other electronic format see DOI: [10.1039/c6dt02709a](https://doi.org/10.1039/c6dt02709a)

used amidinate ligands to examine the dinuclear copper Cu_A site¹⁰ and used the insertion of carbon disulfide into copper–nitrogen bonds to produce polymetallic clusters and control the number of metal ions using the steric properties of the amidinate ligand. Herein, we report the synthesis and characterization of a series of copper complexes with coordination numbers of two, three, and four with linear, trigonal planar and tetrahedral geometries using sulfur and selenium-based terphenyl ligands.

Results and discussion

Dithiocarboxylate complexes

To generate the dithiocarboxylate copper complexes, $(Et_2O)_2Li[S_2C(2,6-(Mes)_2C_6H_3)]$ (Mes = 2,4,6-Me₃C₆H₂)¹¹ and $(thf)_2Li[S_2C(2,6-(Trip)_2C_6H_3)]$ (Trip = 2,4,6-iPr₃C₆H₂)¹¹ were reacted with $[Cu(NCCH_3)_4]PF_6$. The reaction of $(Et_2O)_2Li[S_2C(2,6-(Mes)_2C_6H_3)]$ with $[Cu(NCCH_3)_4]PF_6$ results in an immediate color change from orange to dark brown. After workup, the product, $Cu_4[S_2C(2,6-Mes)_2C_6H_3]_4$, **1**, could be isolated as a brown solid in moderate yield, eqn (1). The reaction of $(thf)_2Li[S_2C(2,6-(Trip)_2C_6H_3)]$ with $[Cu(NCCH_3)_4]PF_6$ also resulted in an immediate color change to dark brown, eqn (2), and $Cu_2[S_2C(2,6-Trip)_2C_6H_3]_2(NCCH_3)_2$, **2**, was recovered as a brown solid. Unfortunately, **2** could not be obtained in acceptable purity for further characterization and we note that if a non-coordinating solvent such as toluene is used for recrystallization, a different product is obtained, but we have been unable to identify the resulting compound.

The reaction of complex **1** with four equivalents of triethylphosphine (PEt₃) yields two products: $Cu_2[S_2C(2,6-$

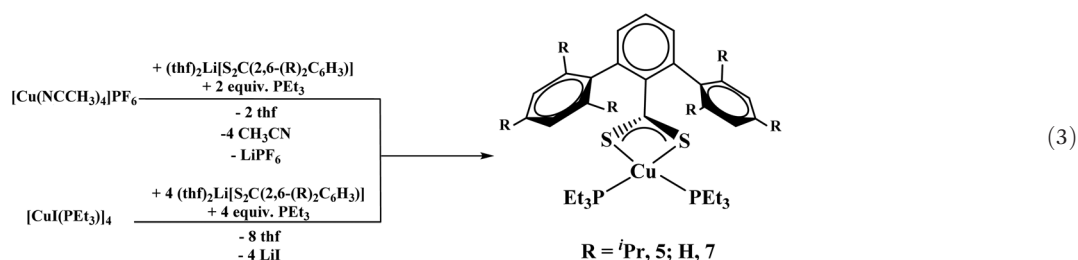
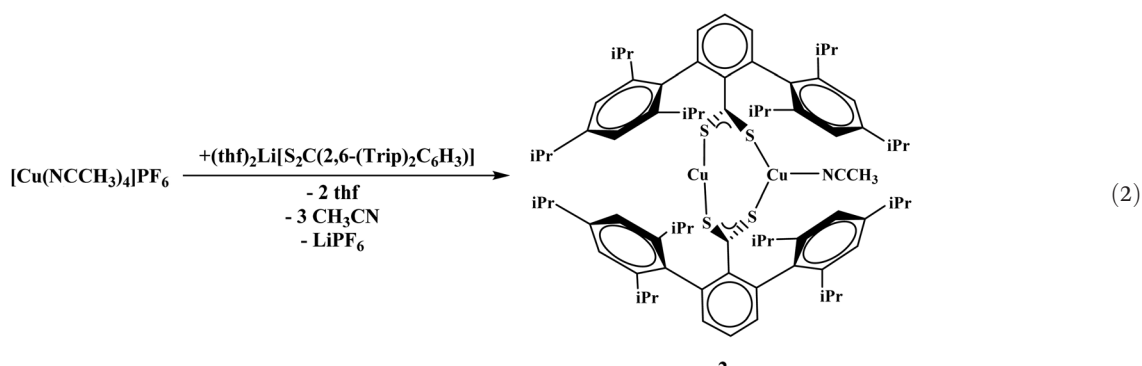
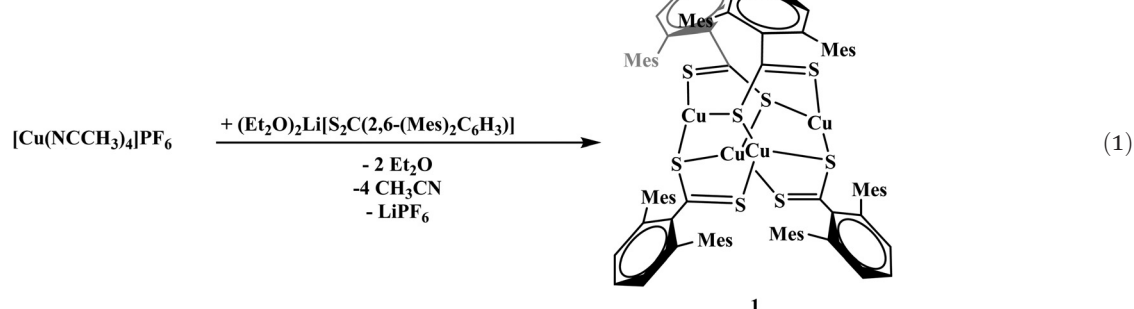
Mes₂C₆H₃)₂(PET₃)₂

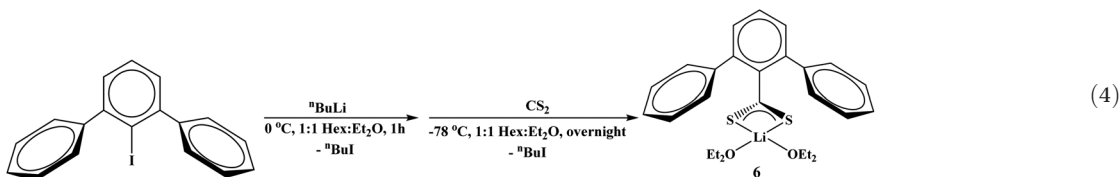
, **3**, and $Cu[S_2C(2,6-Mes)_2C_6H_3](PET_3)_2$, **4**, Scheme 1. During the course of the reaction of **1** with PEt₃, a color change from brown to orange could be observed. Complex **4** could also be synthesized from adding PEt₃ to **3**. To generate complex **3** with an acceptable purity, PEt₃ was pre-installed on the copper center by using $[CuI(PET_3)]_4$, Scheme 1.

The reaction of $(thf)_2Li[S_2C(2,6-(Trip)_2C_6H_3)]$ with $[Cu(NCCH_3)_4]PF_6$ in the presence of two equivalents of PEt₃ or $[CuI(PET_3)]_4$ in the presence of one equivalent of PEt₃ both yielded $Cu[S_2C(2,6-Trip)_2C_6H_3](PET_3)_2$, **5**, in good yield, eqn (3).

Finally, we wanted to examine an unsubstituted terphenyl ligand, which has not been examined as thoroughly as the mesityl and triisopropyl-derivatives. The reaction of 2,6-diphenyliodobenzene with ⁿBuLi followed by addition of CS₂ at -78 °C produced the dithiocarboxylate complex, $(Et_2O)_2Li[S_2C(2,6-Ph)_2C_6H_3]$, **6**, eqn (4). When **6** is reacted with $[Cu(NCCH_3)_4]PF_6$ in the presence of two equivalents of PEt₃, or $[CuI(PET_3)]_4$ in the presence of one equivalent of PEt₃, both yielded **8** in good yield (>75%), eqn (3).

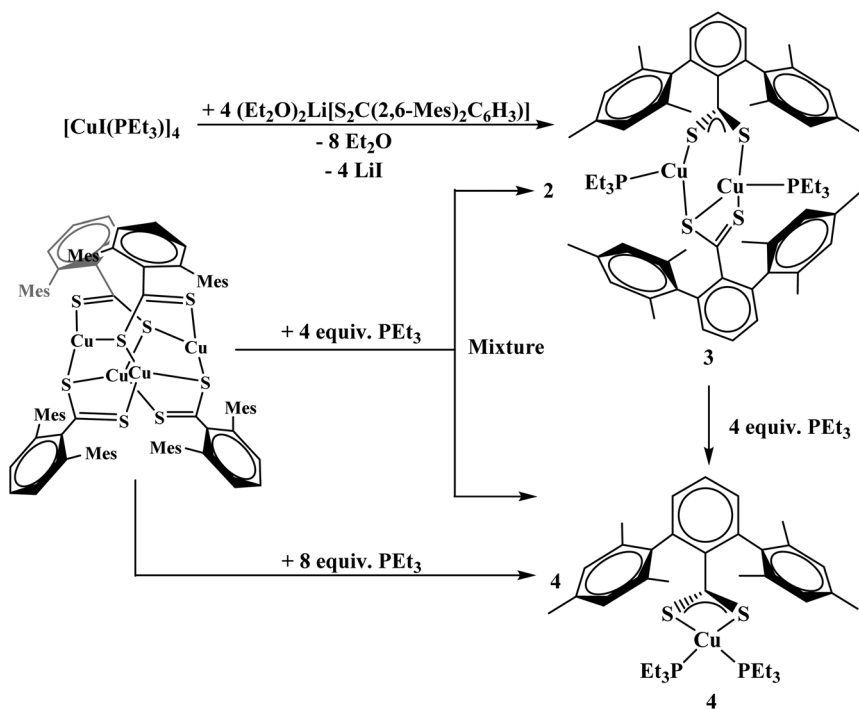
Given that complexes **1**–**5** and **7** could be made from metathesis with dithiocarboxylate salts, we investigated the



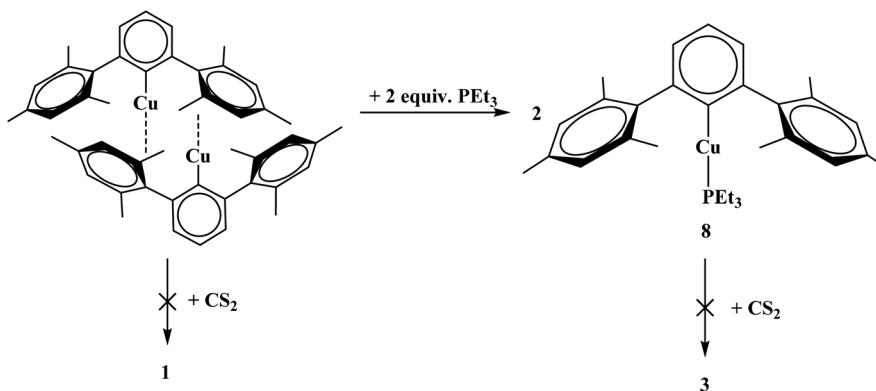


possibility of producing the identical compounds by insertion of CS_2 into the copper–aryl bond of the corresponding terphenyl derivative. Complex **8** is made from $\text{Cu}_2[(2,6\text{-}(4\text{-Mes})_2\text{C}_6\text{H}_3)]_2$ with PEt_3 . However, the reaction of $\text{Cu}_2[(2,6\text{-}(4\text{-Mes})_2\text{C}_6\text{H}_3)]_2$ or $\text{Cu}[2,6\text{-}(4\text{-Mes})_2\text{C}_6\text{H}_3](\text{PEt}_3)$, **8**, with CS_2 to generate copper–sulfur containing complexes did not yield the desirable product, Scheme 2. In fact, no reaction was obtained with either **8** or $\text{Cu}_2[(2,6\text{-}(4\text{-Mes})_2\text{C}_6\text{H}_3)]_2$ when reacted with CS_2 . The

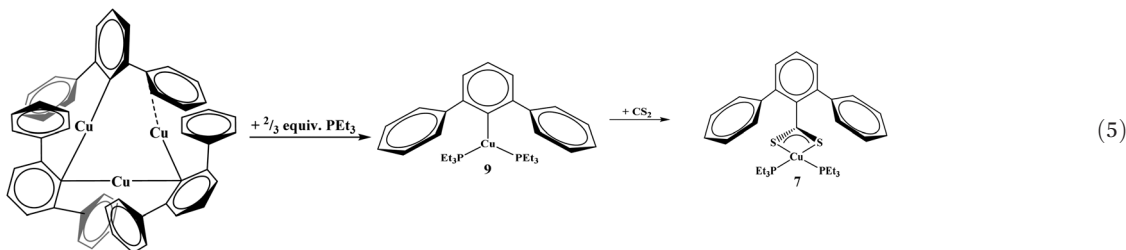
steric bulk of the terphenyl ligand is believed to be the main contributor to the inertness of the complex. When two equivalents of PEt_3 are added to $\text{Cu}_3[(2,6\text{-Ph})_2\text{C}_6\text{H}_3]_3$ ¹² ($\text{Ph} = \text{phenyl}$) in hexanes, $\text{Cu}[2,6\text{-}(4\text{-Ph})_2\text{C}_6\text{H}_3](\text{PEt}_3)_2$, **9**, is produced, eqn (5). However, when **9** is reacted with CS_2 , **7** was isolated, eqn (5). This demonstrates the potential for enhanced reactivity with the unsubstituted terphenyl ligand over their more sterically encumbering counterparts.



Scheme 1 Synthesis of **3** and **4**.



Scheme 2 Synthesis of **8** from $\text{Cu}_2[(2,6\text{-}(4\text{-Mes})_2\text{C}_6\text{H}_3)]_2$ and reactivity toward carbon disulfide (CS_2) towards both complexes.



Chalcogenide complexes

To examine differences in dithiocarboxylate *versus* chalcogenide ligands, the thiolate and selenolate salts were synthesized. The reaction of $[\text{Cu}(\text{NCCH}_3)_4]\text{PF}_6$ and $\text{K}[\text{S}(2,6\text{-Mes})_2\text{C}_6\text{H}_3]$ proceeded with no color change and afforded $\text{Cu}_3[\text{S}(2,6\text{-Mes})_2\text{C}_6\text{H}_3]_3$, **10**, eqn (6). The product could be isolated in nearly quantitative yield (>98%). The reaction of $[\text{Cu}(\text{NCCH}_3)_4]\text{PF}_6$ and $\text{K}[\text{Se}(2,6\text{-Mes})_2\text{C}_6\text{H}_3]$ was carried out in a similar fashion to **10** yielding $\text{Cu}_3[\text{Se}(2,6\text{-Mes})_2\text{C}_6\text{H}_3]_3$, **11**, eqn (6).

With the triisopropyl derivatives, the reaction of $\text{K}[\text{E}(2,6\text{-Trip})_2\text{C}_6\text{H}_3]$ with $[\text{CuI}(\text{PEt}_3)_4]$ yielded mononuclear complexes, $\text{Cu}[\text{E}(2,6\text{-Trip})_2\text{C}_6\text{H}_3](\text{PEt}_3)$, $\text{E} = \text{S}$, **12**; Se , **13**, eqn (7). Without PEt_3 , no product could be readily isolated. Interestingly, all of the chalcogenide complexes, **10–13**, are colorless while the dithiocarboxylate complexes are brown or orange. Reactivity with the unsubstituted terphenyl chalcogenide salts was attempted but yielded multiple products based on the ^1H NMR spectrum which could not be readily discriminated.

All complexes were characterized using ^1H and ^{13}C NMR spectroscopy and, when appropriate, ^{31}P and ^{77}Se NMR spectroscopy, Table 1. The ^{77}Se NMR resonance for $\text{Cu}_3[\text{Se}(2,6\text{-Mes})_2\text{C}_6\text{H}_3]_3$ was observed at -96.2 ppm while **13** showed a resonance at 171.6 ppm. This indicates that the donation from the selenium atom is far greater in **13** with a more down-field chemical shift.

X-ray crystallographic analysis

X-ray structural analysis was used to determine the molecular structure of $\text{Cu}_4[\text{S}_2\text{C}(2,6\text{-Mes})_2\text{C}_6\text{H}_3]_4$, **1**, shown in Fig. 3. All four ligands in the complex are $\mu_3\text{:}\eta^3$ featuring one bridging sulfur and one sulfur which is directly coordinated to one copper atom. The geometry around each copper center could be described as pseudo-trigonal. This is similar to the geometry and coordination environment for copper in the active site of CusA (see Fig. 1). Complex **1** also features two different types of C–S bonds. C(1)–S(1), C(26)–S(3), C(51)–S(6), and C(76)–S(7) all have relatively similar bond distances, $1.7313(18)$, $1.7404(18)$, $1.73820(4)$, and $1.739(2)$ Å, respectively. The average bond distance for all four bonds is 1.737 Å which resembles that of a C–S single bond.¹³ It should also be noted that all four sulfurs are bound to two copper atoms each in a bridging manner. On the other hand, C(1)–S(2), C(26)–S(4), C(51)–S(5), and C(76)–S(8) all have slightly shorter bond

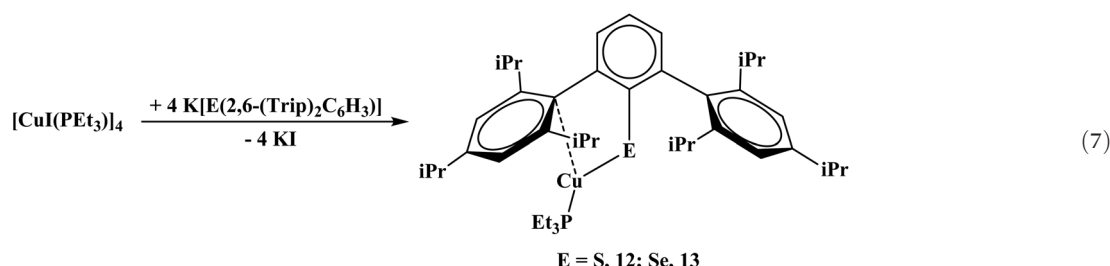
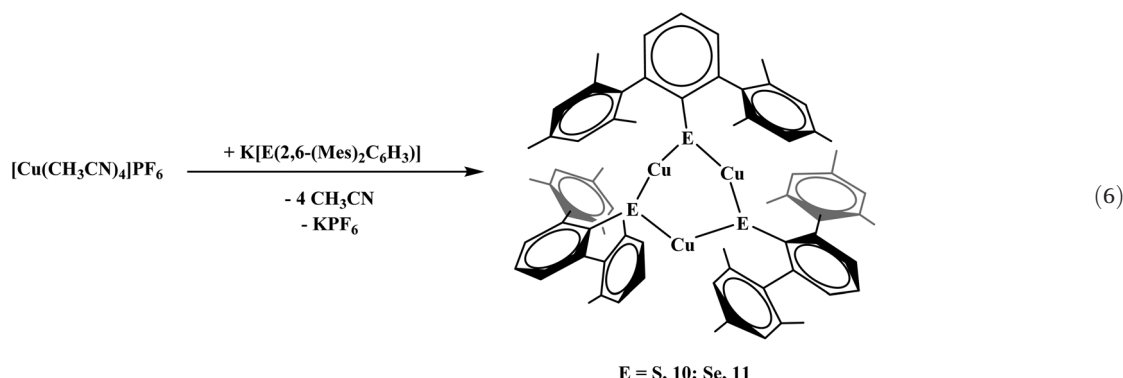


Table 1 Select ^1H , ^{13}C , and ^{31}P NMR resonances (in ppm) for complexes 1, 3–13

Compound	^{13}C NMR CS ₂	^1H NMR						^{31}P NMR
		<i>o</i> -Mes	<i>p</i> -Mes	<i>o</i> -CH(CH ₃) ₂	<i>p</i> -CH(CH ₃) ₂	<i>o</i> -CH(CH ₃) ₂	<i>p</i> -CH(CH ₃) ₂	
Cu ₄ [S ₂ C(2,6-(Mes) ₂ C ₆ H ₃)] ₄ , 1	229.2	2.21	2.16					-8.97
Cu ₂ [S ₂ C(2,6-(Mes) ₂ C ₆ H ₃)] ₂ (PEt ₃) ₂ , 3	246.8	2.43	2.29					-7.01
Cu[S ₂ C(2,6-(Mes) ₂ C ₆ H ₃)](PEt ₃) ₂ , 4	251.7	2.54	2.26					-7.61
Cu[S ₂ C(2,6-(Trip) ₂ C ₆ H ₃)](PEt ₃) ₂ , 5	251.4			1.21, 1.59	1.34	3.44	2.92	-7.73
(Et ₂ O) ₂ Li[S ₂ C(2,6-(Ph) ₂ C ₆ H ₃)] ₂ , 6	251.4							-2.87
Cu[S ₂ C(2,6-(Ph) ₂ C ₆ H ₃)](PEt ₃) ₂ , 7	251.9							-14.49
Cu[(2,6-(Mes) ₂ C ₆ H ₃)](PEt ₃), 8		2.40	2.29					
Cu[(2,6-(Ph) ₂ C ₆ H ₃)](PEt ₃), 9								
Cu ₃ [S(2,6-(Mes) ₂ C ₆ H ₃)] ₃ , 10		2.06	2.24					
Cu ₃ [Se(2,6-(Mes) ₂ C ₆ H ₃)] ₃ , 11		2.07	2.26					
Cu[S(2,6-(Trip) ₂ C ₆ H ₃)](PEt ₃), 12				1.27, 1.60	1.23	3.21	2.80	-9.01
Cu[Se(2,6-(Trip) ₂ C ₆ H ₃)](PEt ₃), 13				1.25, 1.62	1.24	3.18	2.81	-9.51

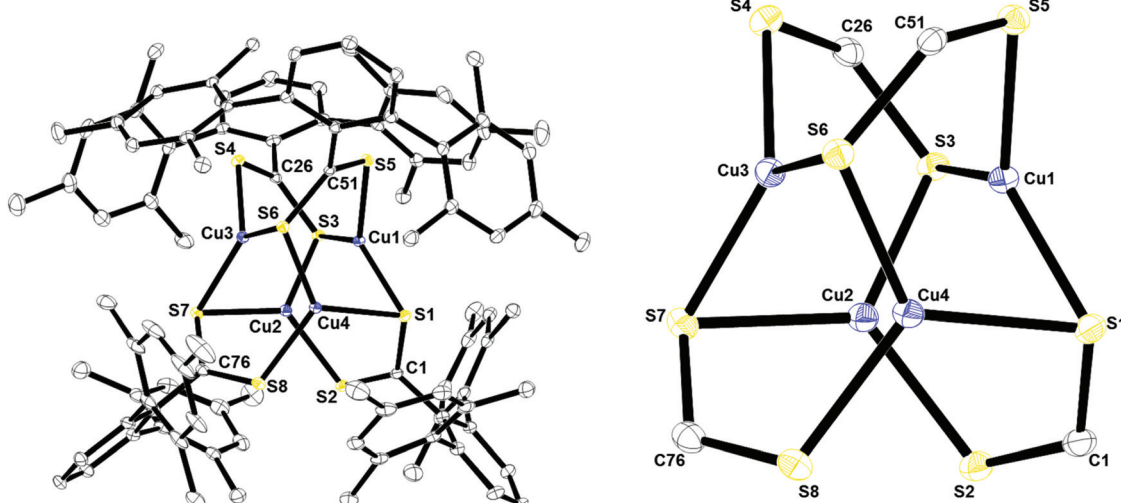


Fig. 3 Thermal ellipsoid plot of 1 shown at the 50% probability level. All hydrogen atoms and residual solvent molecule are omitted for clarity. The Cu₄S₈ core is shown on the right. Selected bond lengths: C1–S1: 1.7313(18) Å; C1–S2: 1.6618(19) Å; C26–S3: 1.7404(18) Å; C26–S4: 1.6580(19) Å; C51–S5: 1.6575(19) Å; C51–S6: 1.73820(4) Å; C76–S7: 1.739(2) Å; C76–S8: 1.660(2) Å; Cu1–S5: 2.2500(5) Å; Cu1–S1: 2.2906(5) Å; Cu1–S3: 2.2907(5) Å; Cu1–Cu2: 2.6029(4) Å; Cu1–Cu4: 2.6113(4) Å; Cu1–Cu3: 2.8575(4) Å.

lengths of 1.6618(19), 1.6580(19), 1.6575(19), 1.660(2) Å, respectively, which resembles a C–S double bond.¹³ This indicates that the anionic charge on the ligand is localized. Interestingly, 1 contains a striking feature in its quaternary carbon resonance on the thiocarboxylate group (229.2 ppm), which was significantly shifted downfield. This localization may be the reason for the observed shift since this is the only compound where localization is observed. The Cu–Cu interactions of 2.6–2.86 Å as well as the Cu–S bond lengths between 2.25–2.30 Å are similar to those observed in other tetranuclear dithiocarboxylate copper(I) clusters.^{14,15}

Fig. 4 shows the crystal structure of 2 obtained from acetonitrile by slow evaporation. The structure features a dinuclear species with a $\mu_2\text{:}\eta^2$ binding mode of the two dithiocarboxylate ligands. One copper, Cu2, is two-coordinate and has a near linear S2–Cu2–S3 bond angle of 169.01(3)°. The other copper

ion, Cu1, is three-coordinate in a pseudo-trigonal geometry. The Cu1–S1 and Cu1–S4 bond distances of 2.2277(5) and 2.2205(5) Å, respectively, are slightly longer than Cu2–S2 and Cu2–S3 of 2.1543(5) and 2.1579(5) Å. This is due to the electron density siphoned by the nitrogen atom of acetonitrile bound to Cu1, which leads to longer copper–sulfur bond distances. The Cu–N(acetonitrile) bond distance is 2.004(2) Å.

The structures of 3 and 4 were determined by X-ray crystallography and revealed dinuclear and mononuclear complexes, respectively. In the solid-state, 3 forms a bimetallic core where the two ligands feature two different binding modes $\mu_2\text{:}\eta^3$ and $\mu_2\text{:}\eta^2$, Fig. 5. Within the $\mu_2\text{:}\eta^2$ unit, the two C–S bonds are essentially the same, indicating that the anionic charge of the ligand is delocalized along the S–C–S unit. The $\mu_2\text{:}\eta^3$ unit features two different C–S bonds. The longer C–S bond in C26–S4 resembles that of a single bond while C26–S3 is close to a



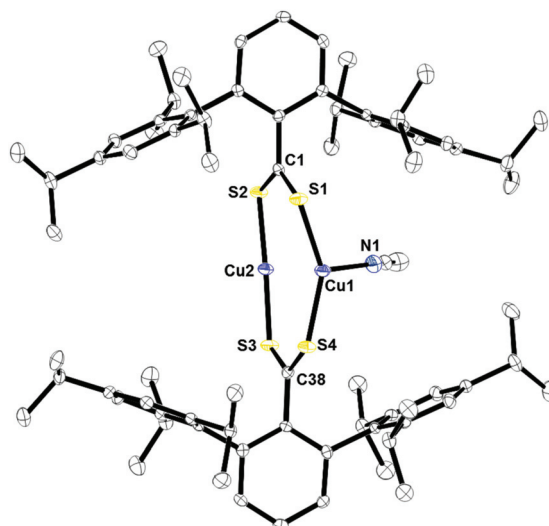


Fig. 4 Thermal ellipsoid plot of **2** shown at the 50% probability plot. All hydrogen atoms are omitted for clarity. Selected bond lengths: C1–S1: 1.6753(19) Å; C1–S2: 1.6912(19) Å; C38–S3: 1.6958(19) Å; C38–S4: 1.6677(19) Å; Cu1–S1: 2.2277(5) Å; Cu1–S4: 2.2205(5) Å; Cu2–S2: 2.1543(5) Å; Cu2–S3: 2.1579(5) Å; Cu1–N1: 2.004(2) Å.

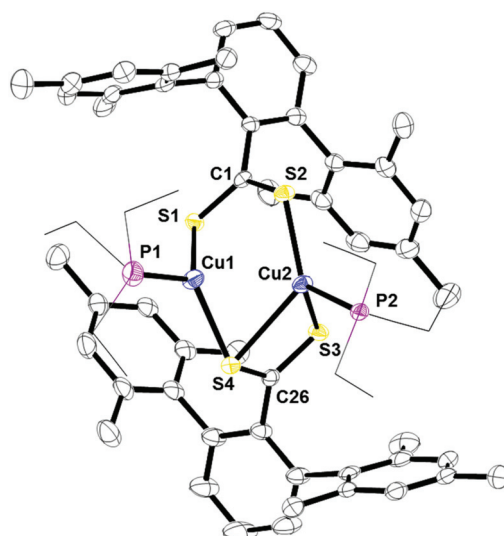


Fig. 5 Thermal ellipsoid plot of **3** shown at the 50% probability level. All hydrogen atoms, carbon atoms on PEt₃, and residue solvent molecule are omitted for clarity. Selected bond lengths: C1–S1: 1.6720(3) Å; C1–S2: 1.6720(3) Å; Cu1–S1: 2.2702(4) Å; Cu2–S2: 2.2440(3) Å; C26–S3: 1.6648(2) Å; C26–S4: 1.7107(3) Å; Cu1–S4: 2.2635(3) Å; Cu2–S4: 2.6307(4) Å; Cu2–S3: 2.3949(7) Å; Cu1–P1: 2.2201(8) Å; Cu2–P2: 2.2243(7) Å.

double bond. Similar to **1**, the sulfur with the longer C–S bond distance is acting as a bridge between two copper centers. Since only one ¹³C NMR resonance is found for the quaternary carbon, the two S–C–S units are the same on the NMR time scale. This type of bonding has been observed in dinuclear copper(I) complexes previously.¹⁶

The structures of **4**, Fig. 6, **5**, Fig. S1,† and **7**, Fig. S2,† are mononuclear copper(I) complexes with pseudo-tetrahedral

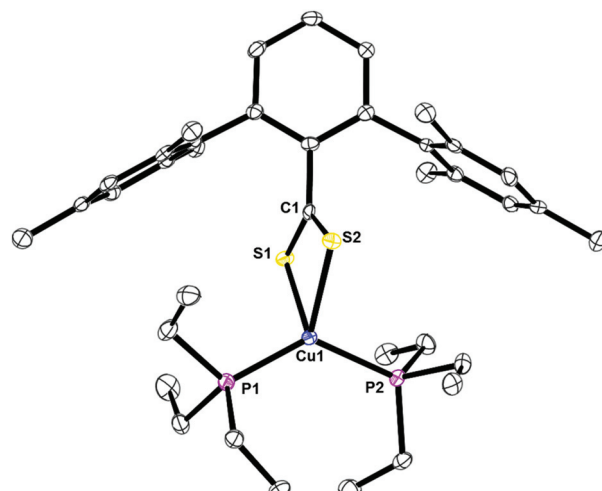


Fig. 6 Thermal ellipsoid plot of **4** shown at the 50% probability level. All hydrogen atoms and residue solvent molecule are omitted for clarity. Selected bond lengths: C1–S1: 1.6795(2) Å; C1–S2: 1.6851(4) Å; Cu1–P1: 2.2175(3) Å; Cu1–P2: 2.2360(3) Å; P1–Cu1–P2: 130.71(4)°; S1–Cu1–P1: 112.35(3)°; S2–Cu1–P1: 112.63(4)°; S1–Cu1–S2: 73.60(3)°.

geometry with two sulfur and two phosphorus atoms coordinated. The data collection for **5** was done at 298 K due to a phase transition at low temperature. In all three compounds, the C–S bond lengths are nearly identical, which indicate that the anionic charge of the ligand is delocalized. The copper–sulfur and –phosphorus bond distances and angles are similar to others reported.

Complex **8**, Fig. 7, contains a two-coordinate copper center with a C1–Cu1–P1 bond angle of 168.380(3)°. Cu₂[2,6-(Mes)₂C₆H₃]₂ has been reported with a Cu1–C1 bond distance of 1.927(5) Å.¹² This is nearly identical to the 1.9282(4) Å bond length in **8**. In addition, the analog of **8** with PPh₃ is known and it contains C1–Cu1–P1 bond angle of 168.82(8)° and Cu1–C1 bond distance of 1.922(3) Å.¹⁷ Complex **9**, Fig. 8, is a

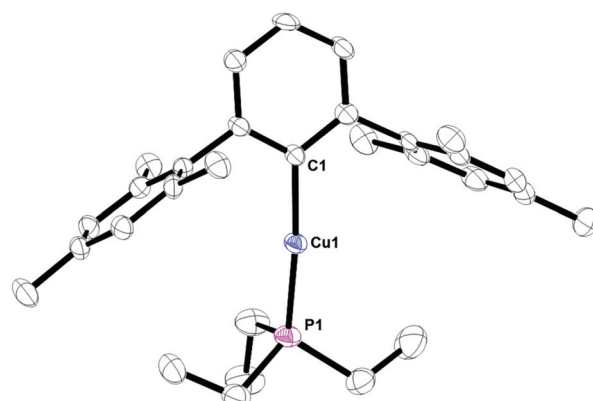


Fig. 7 Thermal ellipsoid plot of **8** shown at the 50% probability level. All hydrogen atoms and residue solvent molecule are omitted for clarity. Selected bond lengths and angles: C1–Cu1: 1.9282(4) Å; P1–Cu1: 2.2003(4) Å; C1–Cu1–P1: 168.380(3)°.

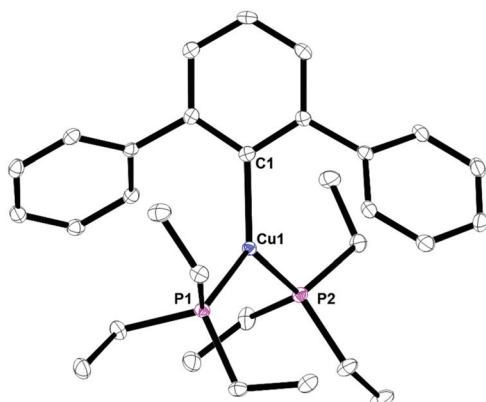


Fig. 8 Thermal ellipsoid plot of **9** shown at the 50% probability level. All hydrogen atoms are omitted for clarity. Selected bond lengths and angles: C1–Cu1: 1.9790(2) Å; Cu1–P1: 2.2495(4) Å; Cu1–P2: 2.558(2) Å; P1–Cu1–P2: 119.526(6)°; C1–Cu1–P2: 119.790(11)°; C1–Cu1–P1: 120.682(6)°.

three-coordinate trigonal planar copper compound with one Cu–C bond of 1.9720(2) Å and all C–Cu–P bond angles of 120°.

Complexes **10**, Fig. 9, and **11**, Fig. S3,† are structural analogs with three copper(i) centers and three mesityl-terphenyl ligands. The geometry around each copper is angular with E–Cu–E (E = S, Se) bond angles between 155–160°. Complex **11** is structurally similar to the previously reported $[\text{Pr}_3\text{PCuSPh}]_3$ ¹⁸ and $(\mu\text{-SPh})_3\text{Cu}_3(\text{PPh}_3)_4$.¹⁹ Few copper–selenium clusters have been reported, but the Cu–Se bond distances in **11** of 2.32 Å are comparable to 2.370(2) to 2.412(2) Å in $[\text{Cu}[\text{Se}(2,4,6\text{-iPr}_3\text{C}_6\text{H}_2)]_6]$.²⁰

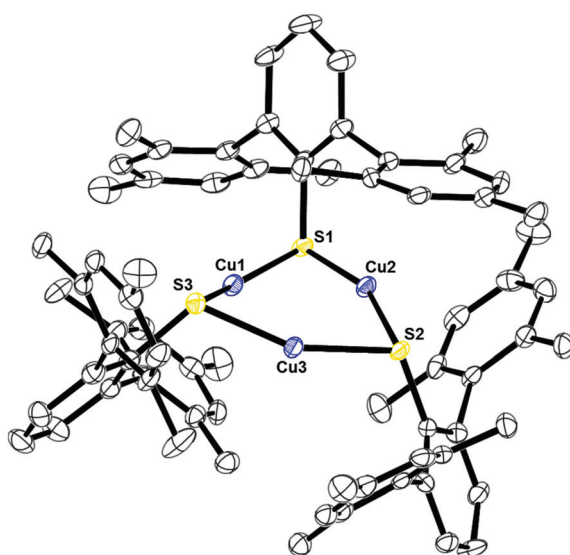


Fig. 9 Thermal ellipsoid plot of **10** shown at the 50% probability level. All hydrogen atoms are omitted for clarity. Selected bond lengths and angles: Cu1–S1: 2.21032(10) Å; Cu2–S1: 2.21033(14) Å; Cu2–S2: 2.22210(13) Å; Cu3–S2: 2.19521(10) Å; Cu3–S3: 2.20693(11) Å; Cu1–S3: 2.20536(11) Å; Cu1–Cu2: 2.92243(16) Å; Cu1–Cu3: 2.85052 Å; Cu3–Cu2: 2.87843(14) Å; S1–Cu1–S3: 155.1371(17)°; S2–Cu3–S3: 157.8052(15)°; S1–Cu2–S2: 159.3547(14)°.

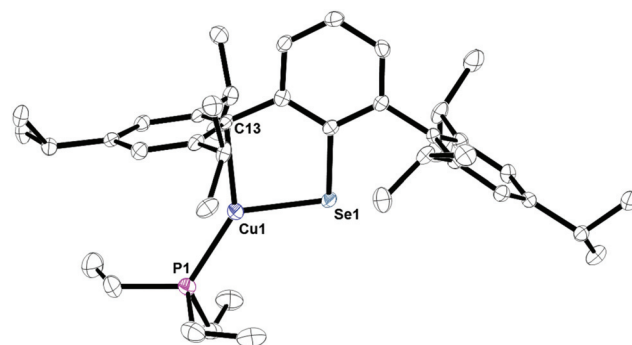


Fig. 10 Thermal ellipsoid plot of **13** shown at the 50% probability level. All hydrogen atoms are omitted for clarity. Selected bond length Cu1–Se1: 2.30182(12) Å; Cu1–C13: 2.28020(12) Å; Cu1–P1: 2.20287(13) Å; Se1–Cu1–C13: 89.276(4)°; C1–Se1–Cu1: 97.56(6)°.

Complexes **12**, Fig. S4,† and **13**, Fig. 10, are three-coordinate complexes which feature the copper center coordinated through a chalcogenide, phosphorus, and an *ipso*-carbon interaction. There is no evidence for the *ipso*-carbon interaction in solution. The Cu1–S1 bond distance of 2.1734(10) Å is close to the 2.1470(8) Å distance in the 3,4,7,8-tetramethyl-1,10-phenanthroline (tmpphen) 2,6-diphenyl-thiophenolatocuppper(i) complex²¹ as well as 2.194(1) Å in (Trip)CuPPh₃.¹⁵ The C1–S1–Cu1 bond angle of 103.53(7)° is comparable to the 102.99(13)° to the corresponding C–S–Cu angle in (Trip)CuPPh₃, but larger than the 98.7(1)° in (tmpphen)Cu[S(2,4,6-Me₃C₆H₂)], tmpphen = 3,4,7,8-tetramethyl-1,10-phenanthroline.²¹ The C1–Se1–Cu1 angle in **13** is larger, 97.56(6)°, due to the larger size of selenium *versus* sulfur. The *ipso*-carbon interactions, Cu1–C13, in **12** and **13** of 2.378(3) and 2.28020(12) Å are similar to those seen in $[\text{Cu}(2,6\text{-}(\text{Mes})_2\text{C}_6\text{H}_3)]_2$ of 2.295(4) and 2.123(4) Å or 2.298(2) and 2.271(2) Å in $[\text{Cu}(\text{C}_6\text{F}_5)]_4(\eta^2\text{-toluene})_2$.²²

Conclusion

We have synthesized twelve new copper(i) complexes with chalcogen-substituted terphenyl-based ligands to produce mono-, di-, tri-, and tetranuclear complexes. This afforded complexes that structurally mimic the active site of several copper-containing proteins such as Atx1 and CusA. The steric properties, in tandem with varying equivalents of PEt₃, forced copper into geometries of near-linear, angular, pseudo-trigonal, and pseudo-tetrahedral. While these geometries are not unusual for copper(i) metal centers, the manipulation of the coordination environment to achieve different geometries is novel and demonstrates the necessity for the large protein manifolds to force the metal centers in alignment for proper function.

In addition, we have synthesized a new lithium dithiocarboxylate terphenyl complex. When the unsubstituted terphenyl ligand was employed, carbon disulfide insertion into the copper–carbon bond was observed, while this was not the case with the mesityl and triisopropyl-derivatives. The chemistry of the terphenyl ligand has been largely unexplored compared to

the mesyl and triisopropyl-derivatives and the coordination chemistry and reactivity of this species is under further investigation.

Experimental

General considerations

All syntheses were carried out under a dry N_2 atmosphere using standard glovebox and Schlenk line techniques. Organic solvents were obtained from Acros and Sigma Aldrich and dried by standard procedures. Potassium *tert*-butoxide (Fisher), $[\text{Cu}(\text{NCCH}_3)_4]\text{PF}_6$ and 10 wt% triethylphosphine (PET_3) in hexane (Strem), potassium bis(trimethylsilyl)amide, carbon disulfide, and 2.5 M *n*-butyllithium (Aldrich) were purchased. $\text{Cu}_2[(2,6-(\text{Mes})_2\text{C}_6\text{H}_3)]_2$,¹² $(\text{Et}_2\text{O})_2\text{Li}[\text{S}_2\text{C}(2,6-(\text{Mes})_2\text{C}_6\text{H}_3)]$,¹¹ $(\text{thf})_2\text{Li}[\text{S}_2\text{C}(2,6-(\text{Trip})_2\text{C}_6\text{H}_3)]$,¹¹ $\text{HS}(2,6-(\text{Mes})_2\text{C}_6\text{H}_3)$,²³ $\text{HSe}(2,6-(\text{Mes})_2\text{C}_6\text{H}_3)$,²⁴ $[\text{CuI}(\text{PET}_3)]_4$,²⁵ $\text{K}[\text{S}(2,6-(\text{Trip})_2\text{C}_6\text{H}_3)]$,²³ $\text{K}[\text{Se}(2,6-(\text{Trip})_2\text{C}_6\text{H}_3)]$,²⁶ 2,6-(Ph)₂C₆H₃I (Ph = C₆H₅),²⁷ and $\text{Cu}_3[(2,6-(\text{Ph})_2\text{C}_6\text{H}_3)]_3$ ¹² were prepared as previously described. $\text{K}[\text{Se}(2,6-(\text{Mes})_2\text{C}_6\text{H}_3)]$ and $\text{K}[\text{S}(2,6-(\text{Mes})_2\text{C}_6\text{H}_3)]$ were made from the following procedure: $\text{K}[\text{S}(2,6-(\text{Mes})_2\text{C}_6\text{H}_3)]$ was generated from $\text{HS}(2,6-(\text{Mes})_2\text{C}_6\text{H}_3)$ and potassium *tert*-butoxide. The reaction was done in *thf* at room temperature for 1 hour, followed by removal of solvent *in vacuo* to yield solid $\text{K}[\text{S}(2,6-(\text{Mes})_2\text{C}_6\text{H}_3)]$. $\text{K}[\text{Se}(2,6-(\text{Mes})_2\text{C}_6\text{H}_3)]$ was generated from $\text{HSe}(2,6-(\text{Mes})_2\text{C}_6\text{H}_3)$ and potassium bis(trimethylsilyl)amide in toluene. Solid $\text{K}[\text{Se}(2,6-(\text{Mes})_2\text{C}_6\text{H}_3)]$ was separated from solution by centrifugation and dried *in vacuo*. Acetonitrile-*d*₃ and benzene-*d*₆ (Cambridge Isotope Laboratories) were dried over molecular sieves and degassed with three freeze–evacuate–thaw cycles. All ¹H and ¹³C{¹H} NMR data were obtained from 500 MHz and 600 MHz DRX Bruker spectrometer. All ⁷⁷Se and ⁷Li NMR data were obtained from 300 MHz DRX Bruker spectrometer. All ³¹P NMR data were obtained from 250 MHz and 300 MHz DRX Bruker spectrometer. ¹H NMR shifts given were referenced internally to the residual solvent peaks at δ 7.16 ppm for C₆D₅H and 7.26 ppm for CHCl₃. All ³¹P NMR shifts given were referenced externally to 85% H₃PO₄ at 0 ppm. All ⁷⁷Se NMR shifts given were referenced externally to diphenyldiselenide in CDCl₃ at 463 ppm. All ⁷Li NMR shifts given were referenced externally to 1 M solution of LiCl in D₂O at 0 ppm. Infrared spectra were recorded as KBr pellets on Perkin-Elmer Spectrum One FT-IR spectrometer. UV-Vis spectra were recorded on a Varian CARY 100 Bio spectrophotometer. Elemental analyses were performed by Atlantic Microlabs, Inc. (Norcross, GA).

Synthesis of Cu₄[S₂C(2,6-(Mes)₂C₆H₃)]₄, 1. In a 20 mL scintillation vial, 2.5 mL of *thf* was added to $[\text{Cu}(\text{NCCH}_3)_4]\text{PF}_6$ (68 mg, 0.18 mmol) followed by 7.5 mL of $(\text{Et}_2\text{O})_2\text{Li}[\text{S}_2\text{C}(2,6-(\text{Mes})_2\text{C}_6\text{H}_3)]$ (100 mg, 0.18 mmol) in *thf* to yield a dark brown colored solution. The mixture was stirred at room temperature overnight after which the solvent was removed *in vacuo*. The brown solid was extracted with toluene then filtered through Celite and the solvent was removed *in vacuo* to yield a brown powder (60 mg, 72%). X-ray quality crystals were obtained from a concentrated *thf* solution at -24 °C. ¹H NMR (600 MHz,

C₆D₆): δ 2.16 (s, 24H, *p*-Mes), 2.21 (s, 48H, *o*-Mes), 6.83 (s, 16H, *m*-Mes), 6.89 (d, 8H, $^3J_{H-H} = 7.2$ Hz, *m*-C₆H₃), 7.07 (t, 4H, $^3J_{H-H} = 7.2$ Hz, *p*-C₆H₃). ¹³C{¹H} NMR (C₆D₆): δ 21.4, 21.5, 128.3, 129.3, 129.6, 136.5, 137.1, 137.2, 137.9, 145.5, 229.2. IR (KBr, cm⁻¹): 2956 (m), 2917 (s), 2855 (w), 1611 (w), 1567 (w), 1449 (s), 1376 (w), 1263 (w), 1099 (s), 1018 (vs), 885 (w), 849 (s), 806 (w), 758 (w), 737 (w), 580 (w), 470 (w). Anal. Calcd for C₁₀₄H₁₁₀OCu₄S₈: C, 66.21; H, 5.88. Found: C, 66.73; H, 5.87.

Synthesis of Cu₂[S₂C(2,6-(Trip)₂C₆H₃)]₂(NCCH₃), 2. The synthesis was carried out in a similar manner to Cu₄[S₂C(2,6-(Mes)₂C₆H₃)]₄ with $[\text{Cu}(\text{NCCH}_3)_4]\text{PF}_6$ (65 mg, 0.17 mmol) and $(\text{thf})_2\text{Li}[\text{S}_2\text{C}(2,6-(\text{Trip})_2\text{C}_6\text{H}_3)]$ (100 mg, 0.14 mmol) to yield an orange solid. The crude product was dissolved in acetonitrile, filtered through Celite, and allowed to evaporate at room temperature outside of the glovebox to yield a small amount of Cu₂[S₂C(2,6-(Trip)₂C₆H₃)]₂(NCCH₃) crystals.

Synthesis of Cu₂[S₂C(2,6-(Mes)₂C₆H₃)]₂(PET₃), 3. In a 20 mL scintillation vial, 5 mL of *thf* was added to $(\text{Et}_2\text{O})_2\text{Li}[\text{S}_2\text{C}(2,6-(\text{Mes})_2\text{C}_6\text{H}_3)]$ (100 mg, 0.18 mmol) followed by 5 mL of $[\text{CuI}(\text{PET}_3)]_4$ (57 mg, 0.046 mmol) in *thf* to yield a deep red solution. The mixture was stirred at room temperature overnight after which the solvent was removed *in vacuo*. The deep red solid was extracted with hexanes the filtered through Celite and the solvent was removed *in vacuo* to yield deep red powder (101 mg, 96%). X-ray quality crystals were obtained from a concentrated hexanes solution at -24 °C. ¹H NMR (500 MHz, C₆D₆): 0.83–0.9 (m, 18H, P(CH₂CH₃)₃), 1.02–1.05 (m, 12H, P(CH₂CH₃)₃), 2.29 (s, 12H, *p*-Mes), 2.43 (s, 24H, *o*-Mes), 6.85 (s, 8H, *m*-Mes), 6.92 (d, 4H, $^3J_{H-H} = 7.5$ Hz, *m*-C₆H₃), 7.11 (t, 2H, $^3J_{H-H} = 7.5$ Hz, *p*-C₆H₃). ¹³C{¹H} NMR (C₆D₆): 8.7, 17.1 (d, $^1J_{C-P} = 15$ Hz), 21.5, 22.2, 127.5, 128.4, 129.3, 135.8, 137.1, 137.8, 139.5, 149.8, 246.8. ³¹P{¹H} NMR (C₆D₆, 300 K): δ -8.97. IR (KBr, cm⁻¹): 2962 (vs), 2913 (vs), 2877 (s), 2729 (w), 1610 (w), 1570 (w), 1453 (s), 1376 (m), 1260 (w), 1220 (w), 1180 (w), 1158 (w), 1095 (w), 1019 (vs), 907 (m), 848 (m), 805 (w), 753 (m), 694 (w), 622 (w), 581 (w). Anal. Calcd for C₆₂H₈₀Cu₂P₂S₄: C, 65.17; H, 7.06. Found: C, 65.26; H, 7.33.

Synthesis of Cu[S₂C(2,6-(Mes)₂C₆H₃)](PET₃), 4. In a 20 mL scintillation vial, 5 mL of toluene was added to $[\text{CuI}(\text{PET}_3)]_4$ (57 mg, 0.046 mmol) followed by 10 wt% PET₃ in hexane (217 mg, 0.18 mmol). The solution was then added to a suspension of $(\text{Et}_2\text{O})_2\text{Li}[\text{S}_2\text{C}(2,6-(\text{Mes})_2\text{C}_6\text{H}_3)]$ (100 mg, 0.18 mmol) in toluene. The mixture was stirred at room temperature overnight after which the solution was filtered through Celite and the solvent was removed *in vacuo* to yield orange powder (61 mg, 48%). X-ray quality crystals were obtained from a concentrated toluene solution at -24 °C. ¹H NMR (600 MHz, C₆D₆): δ 0.81–0.86 (m, 18H, P(CH₂CH₃)₃), 1.07–1.11 (m, 12H, P(CH₂CH₃)₃), 2.26 (s, 6H, *p*-Mes), 2.54 (s, 12H, *o*-Mes), 6.88 (s, 4H, *m*-Mes), 6.98 (d, 2H, $^3J_{H-H} = 7.2$ Hz, *m*-C₆H₃), 7.15 (t, 1H, $^3J_{H-H} = 7.2$ Hz, *p*-C₆H₃). ¹³C{¹H} NMR (C₆D₆): 8.6, 17.2 (t, $^1J_{C-P} = 8.4$ Hz), 21.4, 22.2, 127.1, 127.9, 129.1, 135.5, 137.4, 137.7, 139.8, 150.8, 251.7. ³¹P{¹H} NMR (C₆D₆, 300 K): δ -7.01. IR (KBr, cm⁻¹): 3035 (m), 3005 (m), 2957 (vs), 2911 (vs), 2877 (vs), 2727 (w), 1607 (w), 1568 (w), 1483 (w), 1452 (s), 1411 (m), 1374 (s), 1247 (w), 1219 (w), 1180 (w), 1096 (w), 1013 (br-vs),



923 (m), 854 (m), 804 (w), 773 (vs), 749 (vs), 703 (m), 675 (m), 636 (m), 582 (w), 526 (w). Anal. Calcd for $C_{37}H_{55}Cu_1P_2S_2$: C, 64.46; H, 8.04. Found: C, 64.70; H, 7.92.

Synthesis of $Cu[S_2C(2,6-(Trip)_2C_6H_3)](PEt_3)_2$, 5. The synthesis was carried out in a similar manner to $Cu[S_2C(2,6-(Mes)_2C_6H_3)](PEt_3)_2$ with $(thf)_2Li[S_2C(2,6-(Trip)_2C_6H_3)]$ (100 mg, 0.14 mmol), $[CuI(PEt_3)]_4$ (43 mg, 0.04 mmol), and 10 wt% PEt₃ in hexane (166.5 mg, 0.14 mmol) to yield an orange powder of $Cu[S_2C(2,6-(Trip)_2C_6H_3)](PEt_3)_2$ (53 mg, 44%). X-ray quality crystals were obtained from a concentrated hexanes solution at -24 °C. ¹H NMR (600 MHz, C₆D₆): δ 0.8–0.9 (m, 18H, P(CH₂CH₃)₃), 1.06–1.12 (m, 12H, P(CH₂CH₃)₃), 1.21 (d, 12H, $^3J_{H-H}$ = 7.2 Hz, *o*-CH(CH₃)₂), 1.34 (d, 12H, $^3J_{H-H}$ = 7.2 Hz, *p*-CH(CH₃)₂), 1.59 (d, 12H, $^3J_{H-H}$ = 7.2 Hz, *o*-CH(CH₃)₂), 2.92 (sept, 2H, $^3J_{H-H}$ = 7.2 Hz, *p*-CH(CH₃)₂), 3.44 (sept, 4H, $^3J_{H-H}$ = 7.2 Hz, *o*-CH(CH₃)₂), 7.08 (t, 1H, $^3J_{H-H}$ = 7.5 Hz, *p*-C₆H₃), 7.19 (d, 2H, $^3J_{H-H}$ = 7.5 Hz, *m*-C₆H₃), 7.21 (s, 4H, *m*-Trip). ¹³C{¹H} NMR (C₆D₆): δ 8.7, 17.3 (dd, $^1J_{C-P}$ = 8.6 Hz, $^2J_{C-P}$ = 8.4 Hz), 23.4, 23.5, 26.6, 31.6, 34.7, 120.4, 124.6, 130.8, 135.8, 137.6, 147.3, 148.1, 150.1, 251.4. ³¹P{¹H} NMR (C₆D₆, 300 K): δ -7.61. IR (KBr, cm⁻¹): 3050 (m), 2929 (vs), 2962 (vs), 2869 (vs), 1604 (m), 1566 (w), 1458 (s), 1419 (m), 1479 (m), 1360 (m), 1316 (w), 1258 (w), 1166 (w), 1101 (m), 1026 (s), 931 (w), 874 (m), 802 (w), 764 (s), 712 (w), 651 (w), 627 (w), 464 (w), 432 (w), 408 (w). Anal. Calcd for C₄₉H₇₉Cu₁P₂S₂: C, 68.61; H, 9.28. Found: C, 68.32; H, 9.30.

Synthesis of $(Et_2O)_2Li[S_2C(2,6-(Ph)_2C_6H_3)]$, 6. In a Schlenk flask, 20 mL of *n*-hexane and 20 mL of diethylether was added to 2,6-(Ph)₂C₆H₃I (1.0 g, 2.8 mmol). On the Schlenk line, the flask was cooled to 0 °C in an ice bath. 2.5 M *n*-butyllithium (1.2 mL, 3 mmol) was added *via* syringe. Formation of white precipitate was observed immediately. The flask was allowed to stir at 0 °C for an hour. Ice bath was removed and replaced with dry ice/acetone bath. Once the solution reached -70 °C, carbon disulfide (0.2 mL, 3.3 mmol) was added *via* syringe. The flask was then allowed to stir in dry ice/acetone bath overnight. The resulting orange suspension in light orange liquid was dried under vacuum and brought into N₂ glovebox. The residue was partially dissolved in a 1:1 ratio of *n*-hexane and diethyl ether and transferred a 20 mL scintillation vial. The content in the scintillation vial was concentrated and cooled to -24 °C overnight. The product was isolated as an orange powder which was with *n*-hexane and dried under vacuum (859 mg, 66% yield). X-ray quality crystals were obtained from concentrated a *n*-hexane/diethyl ether solution at -24 °C. ¹H NMR (600 MHz, C₆D₆): δ 0.92 (t, 12H, O(CH₂CH₃)₂), 3.12 (q, 8H, O(CH₂CH₃)₂), 7.10 (t, 1H, $^3J_{H-H}$ = 7.8 Hz, *p*-C₆H₃), 7.10–7.13 (m, 2H, *p*-Ph), 7.17–7.20 (m, 4H, *m*-Ph), 7.24 (d, 2H, $^3J_{H-H}$ = 7.8 Hz, *m*-C₆H₃), 7.94–7.95 (m, 4H, *o*-Ph). ¹³C{¹H} NMR (C₆D₆): δ 15.0, 65.9, 125.9, 126.3, 127.5, 130.0, 130.5, 136.7, 143.6, 154.9, 259.9. ⁷Li{¹H} NMR (C₆D₆, 297 K): -0.17. IR (KBr, cm⁻¹): 3054 (m), 3027 (w), 2974 (s), 2931 (m), 2884 (m), 1597 (w), 1494 (m), 1439 (m), 1385 (m), 1221 (w), 1178 (w), 1154 (w), 1091 (s), 1065 (s), 1021 (vs), 999 (s), 967 (w), 914 (m), 776 (s), 759 (vs), 698 (vs), 613 (m), 530 (w). Anal. Calcd for C₂₇H₃₃Li₁O₁: C, 70.40; H, 7.22. Found: C, 70.42; H, 7.09.

Synthesis of $Cu[S_2C(2,6-(Ph)_2C_6H_3)](PEt_3)_2$, 7. The synthesis was carried out in a similar manner to $Cu[S_2C(2,6-(Mes)_2C_6H_3)](PEt_3)_2$ with $(Et_2O)_2Li[S_2C(2,6-(Ph)_2C_6H_3)]$ (100 mg, 0.22 mmol), $[CuI(PEt_3)]_4$ (67 mg, 0.05 mmol), and 10 wt% PEt₃ in hexane (257 mg, 0.22 mmol) to yield an orange powder of $Cu[S_2C(2,6-(Ph)_2C_6H_3)](PEt_3)_2$ (66 mg, 50%). X-ray quality crystals were obtained from a concentrated *n*-hexane solution at -24 °C. ¹H NMR (600 MHz, C₆D₆): δ 0.83 (s, 18H, P(CH₂CH₃)₃), 1.12 (q, 12H, P(CH₂CH₃)₃), 7.06 (t, 1H, $^3J_{H-H}$ = 7.2 Hz, *p*-C₆H₃), 7.07–7.17 (m, 2H, *p*-Ph), 7.17 (d, 2H, $^3J_{H-H}$ = 7.2 Hz, *m*-C₆H₃), 7.20–7.22 (m, 4H, *m*-Ph), 7.91–7.92 (m, 4H, *o*-Ph). ¹³C{¹H} NMR (C₆D₆): δ 8.5, 17.2, 125.9, 126.3, 127.4, 130.1, 130.9, 138.4, 143.8, 151.6, 251.9. ³¹P{¹H} NMR (C₆D₆, 300 K): -7.73. IR (KBr, cm⁻¹): 3053 (w), 3025 (w), 2960 (s), 2978 (s), 2901 (s), 2872 (s), 2820 (w), 1598 (w), 1572 (w), 1492 (w), 1451 (s), 1416 (m), 1375 (m), 1251 (w), 1232 (w), 1178 (w), 1153 (w), 1094 (w), 1024 (vs), 926 (m), 839 (w), 802 (w), 757 (vs), 694 (vs), 615 (m), 532 (m). Anal. Calcd for C₃₁H₄₃Cu₁S₂P₂: C, 61.51; H, 7.16. Found: C, 61.07; H, 7.10.

Synthesis of $Cu[(2,6-(Mes)_2C_6H_3)](PEt_3)$, 8. In a 20 mL scintillation vial, 5 mL of hexanes was added to $Cu_2[(2,6-(Mes)_2C_6H_3)]_2$ (43 mg, 0.057 mmol) followed by 0.1 mL of 10 wt% PEt₃ in hexane. The mixture was stirred at room temperature overnight after which the solution was filtered through Celite and the solvent was removed *in vacuo* to yield a white powder (44 mg, 78%). X-ray quality crystals were obtained from a concentrated hexanes solution at -24 °C. ¹H NMR (600 MHz, C₆D₆): δ 0.48 (dt, 9H, $^3J_{H-P}$ = 16.8 Hz, $^3J_{H-H}$ = 7.8 Hz, P(CH₂CH₃)₃), 0.61–0.66 (m, 6H, P(CH₂CH₃)₃), 2.29 (s, 6H, *p*-Mes), 2.40 (s, 12H, *o*-Mes), 6.93 (s, 4H, *m*-Mes), 7.22 (d, 2H, $^3J_{H-H}$ = 7.8 Hz, *m*-C₆H₃), 7.42 (t, 1H, $^3J_{H-H}$ = 7.8 Hz, *p*-C₆H₃). ¹³C{¹H} NMR (C₆D₆, 298 K): 8.7 (d, $^2J_{C-P}$ = 2.4 Hz), 16.3 (d, $^1J_{C-P}$ = 21.9 Hz), 21.2, 22.1, 124.3, 125.7, 128.0, 134.2, 136.2, 147.4, 151.0, 169.3. ³¹P{¹H} NMR (C₆D₆, 300 K): δ -2.87. IR (KBr, cm⁻¹): 3027 (m), 2963 (vs), 2933 (vs), 2909 (vs), 2725 (w), 1607 (m), 1544 (m), 1446 (s), 1374 (m), 1233 (m), 1163 (w), 1077 (m), 1034 (s), 850 (m), 796 (m), 762 (m), 729 (m), 579 (w), 548 (w). Anal. Calcd for C₃₀H₄₀Cu₁P₂: C, 72.77; H, 8.14. Found: C, 72.10; H, 8.22.

Synthesis of $Cu[(2,6-(Ph)_2C_6H_3)](PEt_3)_2$, 9. The synthesis was carried out in a similar manner to $Cu[(2,6-(Mes)_2C_6H_3)](PEt_3)$ with $Cu_3[(2,6-(Ph)_2C_6H_3)]_3$ (77 mg, 0.09 mmol) and 10 wt% PEt₃ in hexane (313 mg, 0.26 mmol) to yield a light yellow powder of $Cu[(2,6-(Ph)_2C_6H_3)](PEt_3)_2$ (82 mg, 59%). X-ray quality crystals were obtained from a concentrated *n*-hexane solution at -24 °C. ¹H NMR (600 MHz, C₆D₆): δ 0.74 (dt, 18H, P(CH₂CH₃)₃, $^3J_{H-P}$ = 15 Hz, $^3J_{H-H}$ = 7.8 Hz), 0.99–1.02 (m, 12H, P(CH₂CH₃)₃), 7.05–7.20 (m, 2H, *p*-Ph), 7.29–7.31 (m, 4H, *m*-Ph), 7.42 (t, 1H, $^3J_{H-H}$ = 7.8 Hz, *p*-C₆H₃), 7.72 (d, 2H, $^3J_{H-H}$ = 7.8 Hz, *m*-C₆H₃), 7.96–7.97 (m, 4H, *o*-Ph). ¹³C{¹H} NMR (C₆D₆): 8.5 (d, $^2J_{C-P}$ = 4.5 Hz), 17.4 (d, $^2J_{C-P}$ = 10.5 Hz), 124.6, 125.0, 125.1, 128.4, 128.5, 150.9, 152.3, 177.4. ³¹P{¹H} NMR (C₆D₆, 297 K): -14.49. IR (KBr, cm⁻¹): 3073 (m), 3053 (m), 3018 (m), 2962 (s), 2932 (s), 2898 (s), 2873 (s), 2813 (w), 2726 (w), 1593 (m), 1573 (w), 1559 (w), 1490 (m), 1457 (s), 1442 (m), 1430 (m), 1412 (s), 1376 (m), 1285 (w), 1276 (w), 1236 (m), 1154 (w),



1089 (w), 1068 (w), 1026 (s), 903 (w), 798 (w), 751 (vs), 721 (s), 698 (vs), 613 (m), 554 (m), 500 (w), 419 (w). Anal. Calcd for $C_{30}H_{43}Cu_1P_2$; C, 68.09; H, 8.19. Found: C, 67.96; H, 8.04.

Synthesis of $Cu_3[S(2,6-(Mes)_2C_6H_3)]_3$, 10. In a 20 mL scintillation vial, 5 mL of thf was added to $[Cu(NCCH_3)_4]PF_6$ (81 mg, 0.22 mmol) followed by 5 mL of $K[S(2,6-(Mes)_2C_6H_3)]$ (84 mg, 0.22 mmol) in thf to yield a colorless solution. The mixture was stirred at room temperature overnight after which the solvent was removed *in vacuo*. The white solid was extracted with toluene then filtered through Celite and the solvent was removed *in vacuo* to yield white powder in nearly quantitative yield. X-ray quality crystals were obtained from a concentrated toluene/acetonitrile solution at room temperature. 1H NMR (500 MHz, C_6D_6): δ 2.06 (s, 36H, *o*-Mes), 2.24 (s, 18H, *p*-Mes), 6.74 (d, 6H, $^3J_{H-H} = 7.5$ Hz, *m*- C_6H_3), 6.82 (s, 12H, *m*-Mes), 6.91 (t, 3H, $^3J_{H-H} = 7.5$ Hz, *p*- C_6H_3). $^{13}C\{^1H\}$ NMR (C_6D_6): δ 21.3, 21.7, 125.9, 129.1, 129.7, 135.3, 135.9, 136.7, 139.8, 144.4. IR (KBr, cm^{-1}): 3031 (m), 2968 (s), 2913 (vs), 2853 (s), 2727 (w), 1609 (s), 1569 (m), 1481 (m), 1445 (vs), 1388 (s), 1375 (s), 1113 (w), 1090 (w), 1036 (s), 850 (vs), 798 (s), 771 (w), 741 (vs), 589 (m), 547 (w), 465 (w). Anal. Calcd for $C_{72}H_{75}Cu_3S_3$; C, 70.47; H, 6.16. Found: C, 70.42; H, 6.10.

Synthesis of $Cu_3[Se(2,6-(Mes)_2C_6H_3)]_3$, 11. The synthesis was carried out in a similar manner to $Cu_3[S(2,6-(2,4,6-Me₃C₆H₃))]_3$ with $K[Se(2,6-(Mes)_2C_6H_3)]$ (100 mg, 0.25 mmol) and $[Cu(NCCH_3)_4]PF_6$ (95 mg, 0.25 mmol) to yield an white solid of $Cu_3[Se(2,6-(2,4,6-Me₃C₆H₃))]_3$ (50 mg, 43%). X-ray quality crystals were obtained from concentrated toluene/acetonitrile solution at room temperature. 1H NMR (600 MHz, C_6D_6): δ 2.07 (s, 36H, *o*-Mes), 2.26 (s, 18H, *p*-Mes), 6.71 (d, 6H, $^3J_{H-H} = 7.5$ Hz, *m*- C_6H_3), 6.80 (s, 12H, *m*-Mes), 6.94 (t, 3H, $^3J_{H-H} = 7.5$ Hz, *p*- C_6H_3). 1H NMR (600 MHz, $CDCl_3$): δ 1.88 (s, 36H, *o*-Mes), 2.26 (s, 18H, *p*-Mes), 6.76 (d, 6H, $^3J_{H-H} = 7.8$ Hz, *m*- C_6H_3), 6.82 (s, 12H, *m*-Mes), 7.12 (t, 3H, $^3J_{H-H} = 7.8$ Hz, *p*- C_6H_3). $^{13}C\{^1H\}$ NMR ($CDCl_3$): δ 21.3, 21.4, 126.4, 128.5, 129.2, 130.9, 135.2, 136.7, 140.7, 145.4. $^{77}Se\{^1H\}$ NMR (thf, 297 K): -96.2.

IR (KBr, cm^{-1}): 2912 (vs), 2854 (s), 2726 (w), 1605 (m), 1565 (m), 1443 (vs), 1379 (s), 1271 (w), 1228 (w), 1172 (w), 1093 (w), 1024 (s), 848 (s), 797 (s), 735 (s), 576 (m). Anal. Calcd for $C_{72}H_{75}Cu_3Se_3$; C, 63.22; H, 5.53. Found: C, 63.11; H, 5.64.

Synthesis of $Cu[S(2,6-(Trip)_2C_6H_3)](PEt_3)$, 12. In a 20 mL scintillation vial, 5 mL of thf was added to $[CuI(PEt_3)]_4$ (56 mg, 0.045 mmol) followed by 5 mL of $K[S(2,6-(Trip)_2C_6H_3)]$ (100 mg, 0.18 mmol). The mixture was stirred at room temperature overnight yielding a cloudy white solution after which the solvent was removed *in vacuo*. The white solid was extracted with hexane then filtered through Celite and the solvent was removed *in vacuo* to yield white powder (92 mg, 73%). X-ray quality crystals were obtained from a concentrated hexanes solution at -24 °C. 1H NMR (600 MHz, C_6D_6): δ 0.58 (dt, 9H, $^3J_{H-P} = 16.2$ Hz, $^3J_{H-H} = 7.2$ Hz, $P(CH_2CH_3)_3$), 0.78–0.83 (m, 6H, $P(CH_2CH_3)_3$), 1.23 (d, 12H, $^3J_{H-H} = 6.6$ Hz, *p*- $CH(CH_3)_2$), 1.27 (d, 12H, $^3J_{H-H} = 6.6$ Hz, *o*- $CH(CH_3)_2$), 1.60 (d, 12H, $^3J_{H-H} = 7.2$ Hz, *o*- $CH(CH_3)_2$), 2.80 (sept, 1H, $^3J_{H-H} = 7.2$ Hz, *p*- $CH(CH_3)_2$), 3.21 (sept, 2H, $^3J_{H-H} = 6.6$ Hz, *o*- $CH(CH_3)_2$), 6.94 (t, 1H, $^3J_{H-H} = 7.5$ Hz, *p*- C_6H_3), 7.01 (d, 2H, $^3J_{H-H} = 7.5$ Hz, *m*- C_6H_3), 7.31 (s, 4H, *m*-Trip). $^{13}C\{^1H\}$ NMR (C_6D_6): δ 8.0, 15.6 (d, $^1J_{C-P} = 21$ Hz), 24.1, 24.9, 25.0, 31.3, 34.3, 120.3, 122.4, 128.7, 139.2, 141.2, 146.2, 146.6, 153.6. $^{31}P\{^1H\}$ NMR (C_6D_6 , 297 K): δ -9.01. IR (KBr, cm^{-1}): 3040 (w), 2960 (vs), 2929 (vs), 2867 (s), 2750 (w), 1599 (w), 1565 (w), 1459 (s), 1413 (m), 1383 (s), 1359 (m), 1314 (m), 1254 (w), 1167 (w), 1107 (w), 1075 (w), 1044 (m), 1008 (w), 940 (w), 874 (m), 791 (w), 767 (m), 736 (m), 694 (w), 648 (w), 627 (w), 521 (w). Anal. Calcd for $C_{42}H_{64}Cu_1P_1S_1$; C, 72.53; H, 9.27. Found: C, 72.32; H, 9.47.

Synthesis of $Cu[Se(2,6-(Trip)_2C_6H_3)](PEt_3)$, 13. The synthesis was carried out in a similar manner to $Cu[S(2,6-(Trip)_2C_6H_3)](PEt_3)$ with $K[Se(2,6-(Trip)_2C_6H_3)]$ (93 mg, 0.17 mmol) and $[CuI(PEt_3)]_4$ (51.9 mg, 0.04 mmol) to yield a white solid of $Cu[Se(2,6-(Trip)_2C_6H_3)](PEt_3)$ (71 mg, 42%). X-ray quality crystals were obtained from a concentrated hexanes solution

Table 2 X-ray crystallographic data shown for complexes 1–5

	1	2	3	4	5
CCDC deposit number	1491737	1491738	1491739	1491740	1491741
Empirical formula	$C_{100}H_{100}Cu_4S_8\cdot C_4H_{10}O$	$Cu_7_6H_{101}Cu_2NS_4\cdot C_2H_3N$	$C_{62}H_{80}Cu_2P_2S_4\cdot C_3H_7$	$C_{37}H_{55}CuP_2S_2$	$C_{49}H_{79}CuP_2S_2$
Formula weight (g mol ⁻¹)	1886.55	1324.95	1185.60	689.41	857.72
Crystal habit, color	Plate, red	Prism, orange	Plate, red	Prism, orange	Prism, red
Temperature (K)	100(2)	100(2)	100(2)	100(2)	297(2)
Space group	$P\bar{1}$	Pc	$P\bar{1}$	$P2_1$	$P2_1/n$
Crystal system	Triclinic	Monoclinic	Triclinic	Orthorhombic	Monoclinic
Volume (Å ³)	4634.03(18)	3619.9(4)	3162.1(10)	3628.1(11)	5258.88(19)
a (Å)	13.6538(3)	12.9612(9)	11.944(2)	11.887(2)	13.6652(3)
b (Å)	15.0404(3)	17.4811(12)	13.738(3)	11.899(2)	26.0431(5)
c (Å)	24.7778(6)	16.5758(11)	20.459(4)	25.649(5)	14.8022(3)
α (°)	87.0640(10)	90	84.180(2)	90	90
β (°)	82.3660(10)	105.4550(10)	88.550(2)	90	93.3470(10)
γ (°)	66.7600(10)	90	71.227(2)	90	90
Z	2	2	2	4	4
Calculated density (Mg m ⁻³)	1.352	1.216	1.245	1.262	1.083
Absorption coefficient (mm ⁻¹)	3.080	0.745	0.892	0.830	2.101
Final R indices [$I > 2\sigma(I)$]	$R = 0.0287$	$R = 0.0300$	$R = 0.0401$	$R = 0.0245$	$R = 0.0754$
	$R_w = 0.0697$	$R_w = 0.0788$	$R_w = 0.1027$	$R_w = 0.0574$	$R_w = 0.2458$



Table 3 X-ray crystallographic data shown for complexes 6–11

	6	7	8	9	10	11
CCDC deposit number	1491742	1491743	1491744	1491745	1491746	1491747
Empirical formula	C ₂₇ H ₃₃ LiO ₂ S ₂	C ₆₂ H ₈₆ Cu ₂ P ₄ S ₄	C ₃₀ H ₄₀ CuP	C ₃₀ H ₄₃ CuP ₂	C ₇₂ H ₇₅ Cu ₃ S ₃	C ₇₂ H ₇₅ Cu ₃ Se ₃
Formula weight (g mol ⁻¹)	460.59	1210.50	495.13	529.12	1227.12	1367.82
Crystal habit, color	Prism, yellow	Prism, red	Prism, colorless	Prism, colorless	Prism, colorless	Plate, colorless
Temperature (K)	100(2)	100(2)	100(2)	100(2)	100(2)	100(2)
Space group	P ₂ ₁ /c	P ₂ ₁ /c	P ₂ ₁ /n	Cc	P ₁	P ₁
Crystal system	Monoclinic	Monoclinic	Monoclinic	Monoclinic	Triclinic	Triclinic
Volume (Å ³)	2582.2(6)	6322.2(7)	2710.1(10)	2813.3(9)	2988.2(3)	3027.1(15)
<i>a</i> (Å)	8.8758(12)	17.1313(11)	11.938(3)	15.958(3)	13.0283(6)	13.183(4)
<i>b</i> (Å)	22.935(3)	14.1534(9)	11.356(2)	10.5272(19)	14.0454(7)	14.033(4)
<i>c</i> (Å)	12.6872(17)	26.5086(16)	20.088(4)	17.379(3)	18.6504(9)	18.660(5)
α (°)	90	90	90	90	85.028(4)	85.712(3)
β (°)	91.084(2)	100.3840(10)	95.631(3)	105.505(2)	74.327(4)	73.509(3)
γ (°)	90	90	90	90	65.477(3)	66.271(3)
<i>Z</i>	4	4	4	4	2	2
Calculated density (Mg m ⁻³)	1.185	1.272	1.214	1.249	1.364	1.501
Absorption coefficient (mm ⁻¹)	0.227	0.942	0.880	0.906	1.205	2.890
Final <i>R</i> indices [<i>I</i> > 2σ(<i>I</i>)]	<i>R</i> = 0.0434 <i>R</i> _w = 0.0967	<i>R</i> = 0.0340 <i>R</i> _w = 0.0736	<i>R</i> = 0.0425 <i>R</i> _w = 0.1153	<i>R</i> = 0.0235 <i>R</i> _w = 0.0509	<i>R</i> = 0.0681 <i>R</i> _w = 0.1791	<i>R</i> = 0.0339 <i>R</i> _w = 0.0719

at -24 °C. ¹H NMR (600 MHz, C₆D₆): δ 0.61 (br-s, 9H, P(CH₂CH₃)₃), 0.84 (br-s, 6H, P(CH₂CH₃)₃), 1.24 (d, 12H, ³J_{H-H} = 6.9 Hz, *p*-CH(CH₃)₂), 1.25 (d, 12H, ³J_{H-H} = 6.9 Hz, *o*-CH(CH₃)₂), 1.62 (d, 12H, ³J_{H-H} = 6.9 Hz, *o*-CH(CH₃)₂), 2.81 (sept, 1H, ³J_{H-H} = 6.9 Hz, *p*-CH(CH₃)₂), 3.18 (sept, 2H, ³J_{H-H} = 6.9 Hz, *o*-CH(CH₃)₂), 6.95 (d, 2H, ³J_{H-H} = 7.8 Hz, *m*-C₆H₃), 7.00 (t, 1H, ³J_{H-H} = 7.8 Hz, *p*-C₆H₃), 7.32 (s, 4H, *m*-Trip). ¹³C{¹H} NMR (C₆D₆): δ 8.02, 15.7 (d, ²J_{C-P} = 19.1 Hz), 24.1, 25.0, 25.1, 31.4, 34.3, 121.8, 122.6, 128.3, 140.2, 143.6, 145.7, 146.5, 147.7. ³¹P{¹H} NMR (C₆D₆, 300 K): δ -9.51. ⁷⁷Se{¹H} NMR (C₆D₆, 300 K): δ 171.6 (d, ²J_{Se-P} = 49 Hz). IR (KBr, cm⁻¹): 3042 (w), 2958 (vs), 2929 (vs), 2866 (vs), 2748 (w), 1604 (w), 1594 (w), 1565 (m), 1536 (w), 1459 (s), 1412 (m), 1383 (vs), 1360 (s), 1336 (w), 1314 (m), 1255 (m), 1187 (w), 1167 (w), 1151 (w), 1106 (w), 1079 (w), 1068 (w), 1035 (s), 955 (w), 939 (m), 921 (w), 873 (s), 791 (m), 767 (s), 735 (s), 716 (m), 694 (w), 648 (w), 627 (w), 587 (w), 506 (w), 430 (w). Anal. Calcd for C₄₂H₆₄Cu₁P₁Se₁: C, 67.95; H, 8.69. Found: C, 67.65; H, 8.75.

Crystal structure determination and refinement

The selected single crystal of 1–13 was mounted on a nylon cryoloop using viscous hydrocarbon oil. X-ray data collection was performed at 100(2) K except for 5 which was conducted at room temperature due to a phase transition. The X-ray data were collected on a Bruker CCD diffractometer with monochromated Mo-K α radiation (λ = 0.71073 Å). The data collection and processing utilized Bruker Apex2 suite of programs.²⁸ The structures were solved using direct methods and refined by full-matrix least-squares methods on *F*² using Bruker SHELX-97 program.²⁹ All non-hydrogen atoms were refined with anisotropic displacement parameters. All hydrogen atoms were placed at calculated positions and included in the refinement using a riding model. Thermal ellipsoid plots were prepared by using Olex2³⁰ with 50% of probability displacements for non-hydrogen atoms. Crystal data and details for data col-

Table 4 X-ray crystallographic data shown for complexes 12–13

	12	13
CCDC deposit number	1491748	1491749
Empirical formula	C ₄₂ H ₆₄ CuPS	Cu ₄₂ H ₆₄ CuPSe
Formula weight (g mol ⁻¹)	695.50	742.40
Crystal habit, color	Prism, colorless	Prism, colorless
Temperature (K)	100(2)	100(2)
Space group	P ₂ ₁ /c	P ₂ ₁ /c
Crystal system	Monoclinic	Monoclinic
Volume (Å ³)	4002.0(5)	3980.3(5)
<i>a</i> (Å)	12.9452(8)	12.948(10)
<i>b</i> (Å)	18.3134(12)	17.9243(13)
<i>c</i> (Å)	17.8762(12)	18.0827(14)
α (°)	90	90
β (°)	109.2060(10)	109.0860(10)
γ (°)	90	90
<i>Z</i>	4	4
Calculated density (Mg m ⁻³)	1.154	1.239
Absorption coefficient (mm ⁻¹)	0.664	1.530
Final <i>R</i> indices [<i>I</i> > 2σ(<i>I</i>)]	<i>R</i> ₁ = 0.0400, <i>wR</i> ₂ = 0.1003	<i>R</i> ₁ = 0.0287, <i>wR</i> ₂ = 0.0722

lection for complexes 1–5, 6–11, and 12–13 are provided in Tables 2, 3, and 4, respectively.

Acknowledgements

We gratefully acknowledge the University of Missouri College of Arts & Science Alumni Faculty Incentive Grant and PRIME fund for support of this work.

Notes and references

- P. C. Ford, E. Cariati and J. Bourassa, *Chem. Rev.*, 1999, **99**, 3625–3648.



2 C. Chen, Z. Weng and J. F. Hartwig, *Organometallics*, 2012, **31**, 8031–8037.

3 P. S. Fier, J. Luo and J. F. Hartwig, *J. Am. Chem. Soc.*, 2013, **135**, 2552–2559.

4 J. Rogers, A. B. Dowsett, P. J. Dennis, J. V. Lee and C. W. Keevil, *Appl. Environ. Microbiol.*, 1994, **60**, 1585–1592.

5 J. D. Ranford, P. J. Sadler and D. A. Tocher, *J. Chem. Soc., Dalton Trans.*, 1993, 3393–3399.

6 R. A. Festa and D. J. Thiele, *Curr. Biol.*, 2011, **21**, R877–R883.

7 R. A. Pufahl, C. P. Singer, K. L. Peariso, S.-J. Lin, P. J. Schmidt, C. J. Fahrni, V. C. Culotta, J. E. Penner-Hahn and T. V. O'Halloran, *Science*, 1997, **278**, 853–856.

8 F. Long, C.-C. Su, M. T. Zimmermann, S. E. Boyken, K. R. Rajashankar, R. L. Jernigan and E. W. Yu, *Nature*, 2010, **467**, 484–488.

9 R. C. Fischer and P. P. Power, *Chem. Rev.*, 2010, **110**, 3877–3923.

10 A. C. Lane, C. L. Barnes, W. E. Antholine, D. Wang, A. T. Fiedler and J. R. Walensky, *Inorg. Chem.*, 2015, **54**, 8509–8517.

11 C. Ives, E. L. Fillis and J. R. Hagadorn, *Dalton Trans.*, 2003, 527–531.

12 M. Niemeyer, *Organometallics*, 1998, **17**, 4649–4656.

13 V. K. Shen, D. W. Siderius, W. P. Krekelberg and Eds., *NIST Standard Reference Database Number 101* September 2015 edn., 2015.

14 A. C. Lane, M. V. Vollmer, C. H. Laber, D. Y. Melgarejo, G. M. Chiarella, J. P. Fackler, X. Yang, G. A. Baker and J. R. Walensky, *Inorg. Chem.*, 2014, **53**, 11357–11366.

15 S. Groysman and R. H. Holm, *Inorg. Chem.*, 2009, **48**, 621–627.

16 U. Jayarathne, S. R. Parmelee and N. P. Mankad, *Inorg. Chem.*, 2014, **53**, 7730–7737.

17 M. Niemeyer, *Z. Anorg. Allg. Chem.*, 2003, **629**, 1535–1540.

18 O. Kluge, K. Grummt, R. Biedermann and H. Krautschäid, *Inorg. Chem.*, 2011, **50**, 4742–4752.

19 I. G. Dance, L. J. Fitzpatrick and M. L. Scudder, *J. Chem. Soc., Chem. Commun.*, 1983, 546–548.

20 D. Ohlmann, H. Pritzkow, H. Grutzmacher, M. Anthamatten and R. Glaser, *J. Chem. Soc., Chem. Commun.*, 1995, 1011–1012.

21 A. F. Stange and W. Kaim, *Chem. Commun.*, 1998, 469–470.

22 A. Sundararaman, R. A. Lalancette, L. N. Zakharov, A. L. Rheingold and F. Jäkle, *Organometallics*, 2003, **22**, 3526–3532.

23 M. Niemeyer and P. P. Power, *Inorg. Chem.*, 1996, **35**, 7264–7272.

24 J. J. Ellison, K. Ruhlandt-Senge, H. H. Hope and P. P. Power, *Inorg. Chem.*, 1995, **34**, 49–54.

25 F. G. Mann, D. Purdie and A. F. Wells, *J. Chem. Soc.*, 1936, 1503–1513.

26 M. Niemeyer and P. P. Power, *Inorg. Chim. Acta*, 1997, **263**, 201–207.

27 A. Saednya and H. Hart, *Synthesis*, 1996, 1455–1458.

28 *APEX2 Suite*, Bruker AXS Inc., Madison, Wisconsin, USA, 2007.

29 G. M. Sheldrick, *Acta Crystallogr., Sect. A: Found. Crystallogr.*, 2008, **64**, 112.

30 O. V. Dolomanov, L. J. Bourhis, R. J. Gildea, J. A. K. Howard and H. Puschmann, *J. Appl. Cryst.*, 2009, **42**, 339–341.

